Available online at www.sciencedirect.com
ScienceDirect
Polymer 48 (2007) 4047–4054
polymer
www.elsevier.com/locate/polymer

Spectroscopic and electrical properties of 3-alkyl pyrrole–pyrrole copolymers

Roch Chan Yu King [a], Mourad Boussoualem [b], Frédérick Roussel [b,*]

[a] University of Science and Arts of Oklahoma, Science Division, Chickasha, OK 73018, USA
[b] Laboratoire de Thermophysique de la Matière Condensée, UMR CNRS 8024, MREI, Université du Littoral-Côte d'Opale, 59140 Dunkerque, France

Received 21 February 2007; received in revised form 11 May 2007; accepted 14 May 2007
Available online 21 May 2007

Abstract

Three types of copolymers composed of pyrrole and 3-alkyl pyrroles (with alkyl being pentyl, nonyl and undecyl) have been synthesized. A strong linear dependency of the alkyl chain length on the as-prepared copolymer physical properties is demonstrated via (a) DSC (for phase transition temperatures and enthalpy changes) and (b) UV–vis (for wavelengths of the polaronic and bipolaronic electronic transitions, and ratio of the corresponding absorbances). A trend in the copolymers' doping level vs alkyl chain length is also estimated, via IR, by taking the ratio of band intensities of the stretching modes of the polaronic and bipolaronic species. The copolymers are found to be soluble in organic solvents and their solutions can be cast onto glass substrates or metals resulting in thin films, which can be used as the electroactive component of Schottky diodes. The electrical properties of these diodes are also found to be dependent on increasing 3-alkyl chain length.

Keywords: Semi-conducting polymers; Polaron and bipolaron; Schottky diodes

1. Introduction

Intrinsically conducting polymers (ICPs), e.g., polyanilines and polypyrroles, have been recognized for some time as a class of organic materials capable of exhibiting a unique combination of optical, electrical and magnetic properties. Such uniqueness stems from the ease to controllably and reproducibly modulate, via chemical or electrochemical processes, their doping level so as to reversibly switch them from an insulating to a metallic state [1–4]. While extensive research is still being conducted in improving the properties of ICPs, devices fabricated from this class of materials are known. These include, e.g., biochemical and chemical sensors [5–7], field effect transistors [8,9], actuators [10], all plastic optoelectronic liquid crystal display devices [11], electrostatic protective shields [12] and electrodes for batteries [13]. Among the ICPs, polypyrrole is one of the most investigated because of its good chemical/thermal stability, high conductivity [14] and ease of preparation in a range of solvents. The in situ doping of pyrrole during synthesis produces a p-type semi-conducting material whose electrical property can be traced back to the delocalized polaronic and/or bipolaronic species present in the structure of the heteroaromatic rings.

The well-known insolubility in most common solvents of polypyrrole and its intractability/unmouldability have hampered its processability. Therefore, the scope of practical applications of polypyrroles has been reduced. Nevertheless, recent progress made in the functionalization of pyrrole, via its N-alkylation or C-alkylation at the 3-position of the heterocycle [15] followed by its subsequent polymerization, has led to enhanced solubility of the resulting *N*-alkyl or 3-alkyl polypyrrole. However, the presence of the alkyl side chain in the polymer backbone induces loss of planarity of the aromatic rings due to steric hindrance, thereby reducing its conjugation length and conductivity [16,17].

Although there has been reported work centered on the use of polypyrroles as the electroactive layer for the investigation of electronic properties in Schottky diode metal semi-conducting

* Corresponding author. Tel.: +33 3 2865 8255; fax: +33 3 2865 8241.
E-mail address: frederick.roussel@univ-littoral.fr (F. Roussel).

0032-3861/$ - see front matter © 2007 Elsevier Ltd. All rights reserved.
doi:10.1016/j.polymer.2007.05.039

polymer interface, only a few reports have been published for such use with the *N*-alkylated or *C*-alkylated polypyrrole derivatives [18]. Moreover, a systematic study of the influence of the polypyrrole-alkyl chain length on Schottky diode electrical properties at the metal/polymer interface has not been reported so far.

We reason that one way to maintain a decent degree of ring coplanarity and enhanced polymer solubility is to copolymerize the native pyrrole with a 3-alkylated derivative. In this paper, we report on: (a) the synthesis of three monomeric 3-alkyl pyrroles (with alkyl being pentyl, nonyl and undecyl) followed by their oxidative chemical polymerization with native pyrrole to produce the corresponding, organic solvent soluble copolymers; (b) the formation of semi-conducting films by coating the copolymer solutions onto metallic or glass substrates followed by characterization of the films via DSC, UV–vis and IR spectroscopy; (c) integration of these electroactive films as part of the critical component, i.e., metal/polymer semiconductor interface, of a Schottky diode whose characteristics are investigated by means of current density–voltage (J–V) measurements. The variation in the length of the alkyl chains on the afore-mentioned characteristics is also discussed.

2. Experimental section

2.1. Synthesis of 3-alkyl pyrroles

Pyrrole was vacuum distilled prior to polymerization. The remaining chemicals and solvents (Aldrich Chemical Co.) were used as supplied without further purification.

Several methods for the synthesis of 3-alkyl pyrroles are known. We have adopted the unconventional, less cited synthetic and shorter, albeit lower yielding route of Babler and Spina [19], who in their attempt to prepare α-substituted succinaldehydes, have unexpectedly isolated short chain 3-alkyl (isopropyl or *n*-butyl) pyrroles. These products were isolated during vacuum distillation of crude product. We found that the three-step procedure can also be used for the synthesis of longer 3-alkyl (pentyl, nonyl or undecyl) pyrrole derivatives (Scheme 1). All 3-alkylated pyrrole monomers were concomitantly isolated in a Kugelrohr apparatus during the final vacuum distillation. They were fully characterized by NMR

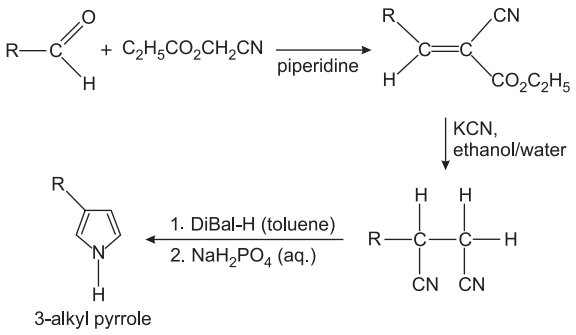

Scheme 1. Synthetic route for 3-alkyl pyrrole (alkyl = pentyl, nonyl or undecyl).

(Varian 300 MHz spectrometer). The ^1H and ^{13}C NMR spectra (Table 1) are from solutions using $CDCl_3$ as the solvent and the chemical shifts quoted are relative to TMS.

2.2. Preparation of copolymers

The copolymerization of 3-alkyl pyrrole and pyrrole was conducted under a blanket of N_2 using a method adapted from the literature with $FeCl_3$ (aq.) as the oxidant [20] and a molar ratio of 3-alkyl pyrrole/pyrrole of 2.50. The copolymer formed was washed with copious amounts of water and then with small amounts acetone until the washings were colorless. This is to ensure the removal of salts, monomers and oligomers. The resulting black powder was then dried in vacuum overnight. The as-prepared copolymers are labelled coPPy-3C*n*PPy, where *n* is the number of carbons of the alkyl side chains. A detailed characterization of coPPy-3C*n*PPy by differential scanning calorimetry (DSC), SEM, UV–vis and IR spectroscopies is presented in Section 3.

2.3. Sample preparation and measurement methods

The preparation of films of 3-alkyl pyrrole (homopolymers) via electrochemical process has been reported [21,22]. We have adopted a different approach which is based on using the chemically prepared copolymers composed of pyrrole and 3-alkyl pyrroles to produce thin films. The following is a typical procedure: a suspension of copolymer (0.030 g) in 10 ml $CHCl_3$ was sonicated for 2–5 h (shorter alkyl chain containing copolymers require longer sonication times) after which time it was suction filtered. The filtrate was slowly reduced approximately to one-third of its initial volume at 50 °C. The remaining solution was used for film preparation via casting onto either glass microscope slides (Menzel Glaser, Germany) for spectral analyses or aluminum vacuum deposition on glass substrate for Schottky diodes' preparation. In the latter case, a gold thin film electrode ($\sim$25 mm^2) was then deposited on top of the copolymer film by vacuum evaporation under 10^{-3} mbar (Cressington Sputter Coater 108), with the gold electrode patterned via suitable masking. The resulting Schottky diodes are referred to as Al/coPPy-3C*n*PPy/Au (with C*n* being the number of carbons in the 3-alkyl side chain). Film thickness was obtained with the use of a micro-caliper (Mitutoyo, Japan). The UV–vis and IR (KBr pellets of pulverized copolymer films) spectra were recorded on a Perkin–Elmer Lambda 2S and a Bruker Equinox 55 spectrometers, respectively. The differential calorimetric measurements were performed on TA Q1000 calorimeter under nitrogen atmosphere (50 ml min^{-1}) with the heating rate set at 10 °C min^{-1}.

2.4. Electrical measurements

The electrical conductivity was determined using both conventional linear four-probe and impedance spectroscopy techniques. Four-probe experiments were carried out on a setup consisting of a Lake Shore 120CS DC current source and

Table 1
Spectral data of 3-alkyl pyrrole monomers

3-Pentyl pyrrole	
^{1}H NMR δ (ppm)	8.10 br s (N–H), 6.71 m (C–H), 6.56 m (C–H), 6.08 m (C–H), 2.47 t (CH_2), 1.67 m ($-(CH_2)_3-$), 0.87 t (CH_3)
^{13}C NMR δ (ppm)	124.96, 117.84, 115.01, 108.82, 32.06, 31.21, 27.21, 22.90, 14.40
3-Nonyl pyrrole	
^{1}H NMR δ (ppm)	8.01 br s (N–H), 6.71 m (C–H), 6.56 m (C–H), 6.08 m (C–H), 2.46 t (CH_2), 1.68 m ($-(CH_2)_7-$), 0.86 t (CH_3)
^{13}C NMR δ (ppm)	124.67, 117.54, 114.78, 108.53, 31.91, 31.23, 29.69, 29.62, 29.57, 29.36, 26.93, 22.68, 14.13
3-Undecyl pyrrole	
^{1}H NMR δ (ppm)	8.00 br s (N–H), 6.71 m (C–H), 6.56 m (C–H), 6.09 m (C–H), 2.47 t (CH_2), 1.67 m ($-(CH_2)_9-$), 0.86 t (CH_3)
^{13}C NMR δ (ppm)	124.63, 117.53, 114.76, 108.48, 31.91, 31.23, 29.69, 29.65, 29.57, 29.34, 26.93, 22.68, 14.11

a Chauvin–Arnoux CA 5240G numeric multimeter [23]. Impedance measurements were performed at room temperature using an HP 4194A impedance/gain phase analyzer. The current density–voltage (J–V) characteristics of Al/coPPy-3C*n*PPy/Au devices were investigated at room temperature with the use of an Agilent E3631A stabilized DC output generator and an HP 34401A digital multimeter.

3. Results and discussion

3.1. Differential scanning calorimetric analyses and morphology of copolymers

Differential calorimetric measurements have been conducted on pelletized samples (5 mg) to assess the thermal stability of the crude copolymers. A typical DSC thermogram recorded on the first heating ramp is given in Fig. 1. According to previous works on polypyrrole derivatives, the broad exothermic peak observed at high temperature ($T > 300$ °C) has been assigned to the thermal decomposition of the copolymers [24]. The exothermic peak detected at lower temperature (~195 °C) was observed during the first heating scan suggesting that this transformation is mainly irreversible. It can also be seen that the corresponding transition temperature measured for the various copolymers appears to be linearly dependent on the number of Cs of the alkyl side chains (inset of Fig. 1, left axis). Furthermore, the enthalpy change increases with increasing alkyl chain length (inset of Fig. 1, right axis). These observations may stem from partial ordering upon heating of aliphatic side chains present as spacers in-between the copolymer backbone. In other words, the heat flow released at ~195 °C could be associated with a cold crystallization process resulting from the conformational changes of the alkyl side chains. However, the thermograms exhibit no observable side chain melting endotherms with temperature rise. This is in accord with previous X-ray and DSC studies on polymers (flexible or rigid backbones) bearing long alkyl chains, indicating that localized side chain order may exist within a predominantly amorphous polymer matrix [25,26].

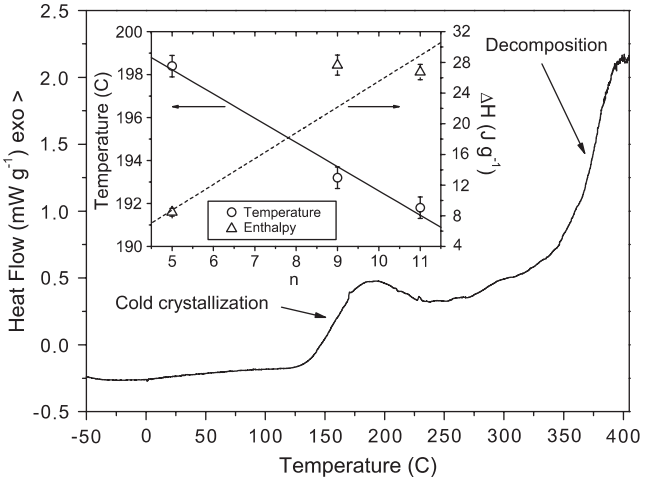

Fig. 1. DSC thermogram of coPPy-3C*11*PPy on heating; inset: temperature (left) and enthalpy change (right) of the cold crystallization process vs alkyl chain length.

SEM experiments were carried out to investigate the influence of the film preparation method on the sample morphology. The as-prepared copolymers (powders) exhibit a cauliflower-like texture with grain size ranging from 50 to 300 nm (Fig. 2a). According to the procedure reported in Section 2, copolymer powders were processed to afford solutions which were then cast with a bar-coater onto conventional microscope glass slides to form thin films. On the right hand side of the SEM picture displayed in Fig. 2b, it can be seen that the top surface of the coPPy-3C*11*PPy film is quite uniform, smooth and flat showing the high quality of the coating. The left hand side of the picture corresponds to the edge of the sample which was initially used to focus on the surface. The edge of the sample exhibits a step-like structure associated with thickness changes in-between micron-sized holes.

3.2. UV–vis spectral analyses of copolymers

A typical electronic absorption spectrum of the copolymer films cast onto glass substrates from $CHCl_3$ solutions is shown in Fig. 3. All spectra present two main absorption bands named λ_1 and λ_2. The peak detected at ~400 nm (λ_1) is characteristic of a benzenoid π–π^* transition absorbance which is the spectral feature of a bipolaron band structure in the copolymers [27,28]. The data indicate that copolypyrroles bearing shorter alkyl side chains exhibit a more pronounced bathochromic (red) shift of the bipolaronic peak (inset of Fig. 3, open diamonds). Thus, a correlation between the alkyl side chain length and electronic transitions from the valence band to the anti-bipolaron (upper polaron) band in this series of

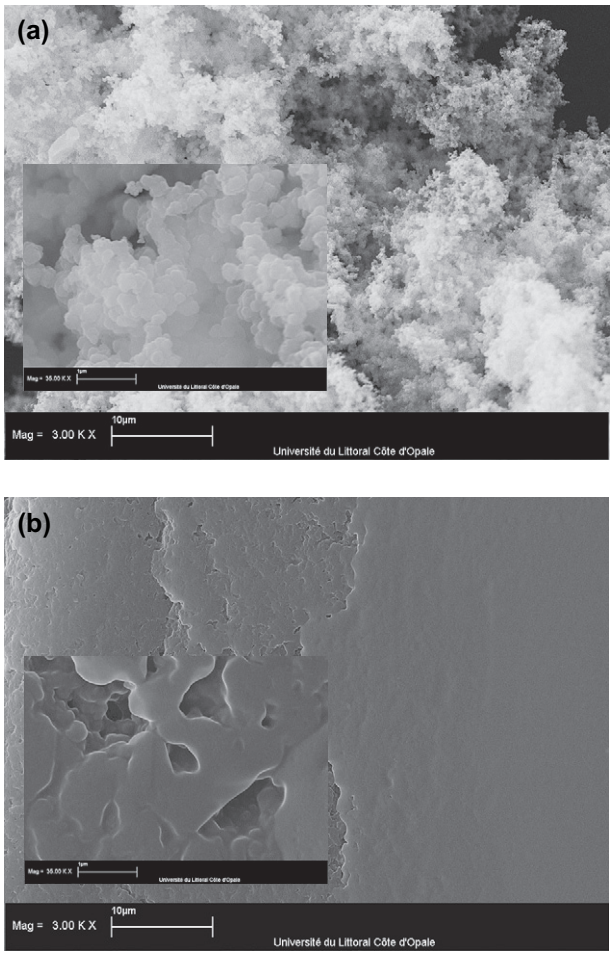

Fig. 2. SEM pictures of coPPy-3C*11*PPy samples: (a) as-synthesized compound and (b) film on a glass substrate obtained after processing of the crude compound (the left hand side of the picture shows the edge of the film); insets: enlarged views (the white scale bar represents 1 μm).

ICPs is obtained. In other words, these transitions are facilitated by the presence of a shorter alkyl chain whose contribution in ring plane distortion, thereby π conjugation length is minimized. The presence of a second peak located within the 600–800 nm range is also observed with a noticeable trend in the bathochromic shift at λ_2 (inset of Fig. 3, solid diamonds) similar in sequence to the afore-mentioned one. Considering previous works on polypyrroles [29,30] and substituted polypyrroles [31–33], this absorption band is ascribed to the electronic transition from the lower polaron to the upper polaron level. Indeed, we surmise that segments of undoped and/or dedoped alkylated pyrrole units are present in the copolymer backbone. These alkylated segments should release more electron density around the neutral N-atom of the undoped/dedoped aromatic rings and their presence also induces a more distorted conformation in the copolymer backbone which in turn affects the electronic transitions from the fully aromatized undoped rings (benzoid) into the conjugated polyene-like moieties (quinoid) [34] of the copolymer backbone, analogous to the benzenoid to quinoid transition observed in polyanilines [35]. In addition to the above spectral features, a free carrier tail extending into the near IR region is also observed. Its

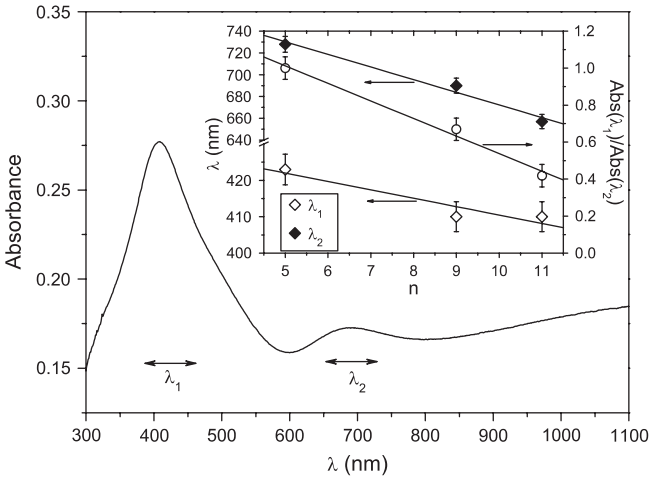

Fig. 3. UV–vis spectrum of a coPPy-3C9PPy film; inset: wavelength (left) and UV absorbance ratio λ_1/λ_2 (right) vs alkyl chain length.

shape indicates the presence of a more relaxed/expanded polymeric chain which can be associated with the delocalized conjugation length, i.e., the length of an intramolecular electronic path in polymer chain [36].

It is also worthwhile to indicate that both the wavelengths λ_1 and λ_2 and the ratio of their absorbances (λ_1/λ_2) are linearly correlated to the number of hydrocarbon units of the alkyl chain as shown in the inset of Fig. 3 (open circles). These results are useful in that they may provide an estimation of the degree of substitution and/or doping level for other closely related copolymers. Thus, the trend in the doping level of copolymers is qualitatively estimated to be as follows: coPPy-3C5PPy > coPPy-3C9PPy > coPPy-3C*11*PPy. Therefore, it can be inferred that the intrinsic copolymer film conductivities would follow the same trend.

3.3. Infrared spectral analyses of copolymers

Infrared spectroscopy of the as-prepared copolymer films was undertaken. Fig. 4 shows a representative IR spectrum

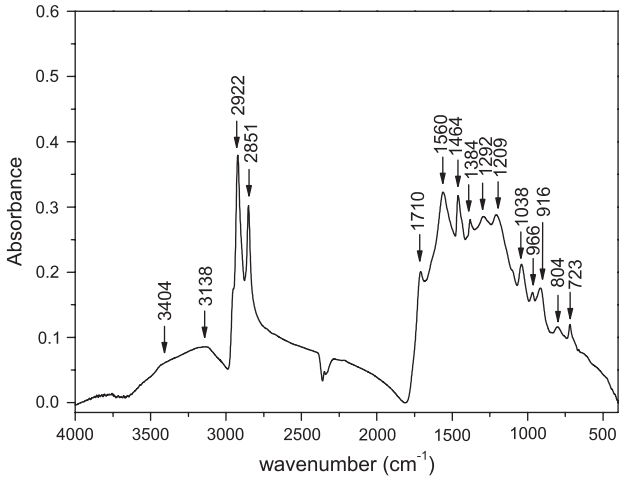

Fig. 4. IR spectrum of coPPy-3C*11*PPy.

of the copolymer (coPPy-3C*11*PPy) based film. Table 2 provides the pertinent band positions (cm^{-1}) of all three as-synthesized copolymers. The locations of bands falling into the regions ~2800 to 2875 cm^{-1} are associated with CH_2 symmetrical stretching modes and those from ~2875 to 2975 cm^{-1} are from CH_2 asymmetrical stretching modes, mixed with a minor absorption at 2965 cm^{-1} which is related to CH_3 stretching. These absorptions may provide some insight into aliphatic chain conformations, defects and packing arrangements. For example, the ratio of band intensities (I_{2850}/I_{2930}) is a diagnostic feature of chain arrangement [37], i.e., the higher the above ratio, the more ordered the chains suggesting that a predominance of *trans* conformations in the methylene (CH_2s) backbone. While there is no detectable frequency shift observed in the symmetrical and asymmetrical vibrational modes in our IR spectra (Table 2 and Fig. 5), however, the ratio of band intensities (inset of Fig. 5) decreases linearly with *n*, showing that an increase in alkyl chain length leads to a lower degree of *trans*-conformational order. This result could be explained by a side chain folding of longer alkyl homologues along the copolymer backbone which requires a *cis*-conformational order to occur. This reflects a better overall structural fit between the copolymer backbone with that of the alkyl chains serving as spacers of aromatic rings.

It is well documented that the conduction process in one-dimensional conjugated polymer chain involves the participation of either polaronic and/or bipolaronic species via hopping between adjacent sites [38,39]. The IR features observed in the spectral region 850–1650 cm^{-1} (Fig. 6) provide some information on the degree of electron delocalization through analyses of the C–C and C–N stretching modes in pyrrole

Table 2
IR spectral characteristics of coPPy-3C*n*PPy

IR absorption band positions (cm^{-1})			Mode
$n=5$	$n=9$	$n=11$	
3440	3443	3404	ν(N–H), stretch secondary amine
3140	3142	3138	ν(=C–H), stretch
2922	2922	2922	$\nu(CH_2)$, asym stretch
2852	2852	2851	$\nu(CH_2)$, sym stretch
1710	1710	1710	ν(C=O), stretch (by-product)
1558	1559	1560	ν(C=C)/(C–C) bipolaron
1459	1461	1464	ν(C=C)/(C–C) polaron
1381	1381	1384	ν Ring + rock CH_3
1292	1291	1292	Ring C–H in-plane bending
1208	1207	1209	Ring breathing
1086	1092	1098	δ(N–H), bending
1041	1036	1038	δ Ring, bending deformation
970	970	966	δ Ring, bending deformation
914	912	916	δ Ring in-plane deformation
804	804	804	δ CH out of plane deformation
–	721	723	ν CH_3 rocking

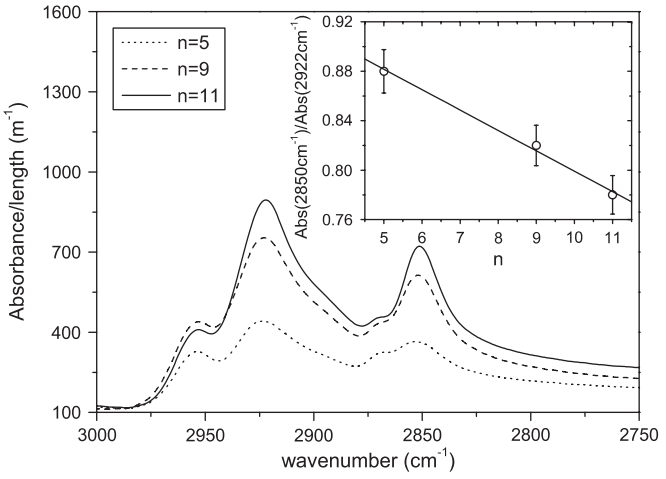

Fig. 5. IR alkyl symmetrical (2850 cm^{-1}) and asymmetrical (2922 cm^{-1}) CH_2 vibrational modes; inset: absorbance ratio vs alkyl chain length.

[40,41]. In particular, the bands located at ~1560 cm^{-1} (bipolaronic band) and 1464 cm^{-1} (polaronic band) indicate that the area change associated with the bipolaronic band is much more dependent on the length of the alkyl side chain than that of the corresponding polaronic band (inset of Fig. 6). Nevertheless, the above spectral finding is approximate because the less prominent polaronic band at 1464 cm^{-1} overlaps to some extent (at right) with that of the alkyl bending modes. Recalling that the degree of electron delocalization in unalkylated polypyrroles is inversely proportional to the ratio of the above-mentioned band areas [42], the trend implies that the copolymer functionalized with shorter alkyl chains exhibits an improved electron delocalization which is in agreement with the UV–vis analyses.

3.4. Measurements of electrical characteristics

The coPPy-3C*n*PPy conductivities were estimated using both linear four-probe and impedance spectroscopy techniques [43]. Fig. 7 displays the plot of the DC conductivity (σ) against

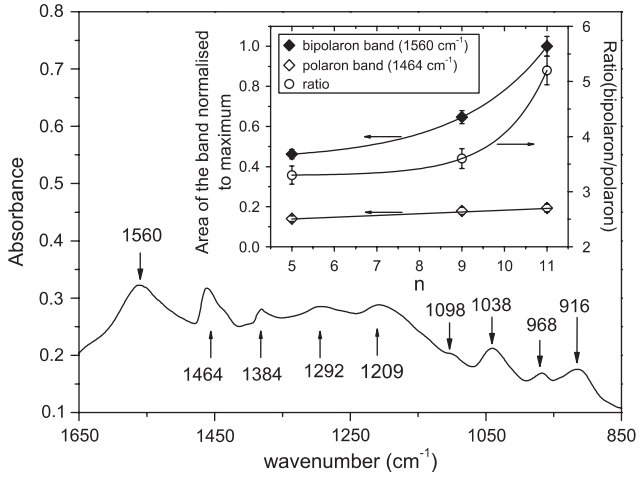

Fig. 6. IR spectrum in the spectral region 850–1650 cm^{-1}; inset: polaron and bipolaron absorption band area (left) and band ratio (right) vs alkyl chain length.

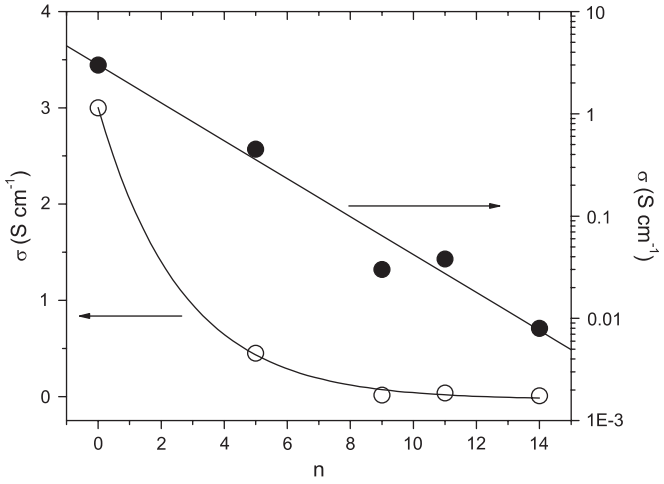

Fig. 7. Influence of the alkyl chain length (n) on the electrical conductivity (σ).

alkyl chain length n (average σ values for $FeCl_3$ doped PPy ($n=0$) [44] and $n=14$ (homopolymer) [18] were taken from the literature and inserted in the plot for comparison purposes). It can be clearly seen that the conductivity drops drastically as n increases (open symbols). Using the variable range hopping model (VRH) proposed by Mott and coworkers [45–47], the conductivity, in the case of a three-dimensional transport, can be expressed [48,49] as:

$$\sigma_{DC} = \sigma_0 \exp\left[-\left(\frac{\lambda}{\xi^3 N_{Ef} kT}\right)^{1/4}\right], \quad (1)$$

where λ is a dimensionless constant, ξ is the delocalization length of the electron wave function ($0.3 < \xi < 1$ nm [43]), N_{Ef} is the density of states at the Fermi level, k is the Boltzmann constant, and T is the temperature. Recalling that our experiments were performed at room temperature, i.e., $T =$ constant, the conductivity can be approximated as:

$$\sigma_{DC} \propto \sigma_0 \exp\left[-\left(\frac{K}{N_{Ef}}\right)^{1/4}\right], \quad (2)$$

where K is a constant. Using a logarithmic-linear scale (right axis, solid symbols), the plot of $\log_{10}(\sigma)$ vs n exhibits a linear decrease indicating that the conductivity obeys a first order-like exponential decay similar to a plot derived from Eq. (2). In other words, an increase in the alkyl side chain length leads to a shift towards a more pronounced semi-conducting regime which might be associated with a decrease in the density of states (induced by an enhanced ring torsion) at the Fermi level (N_{Ef}). This trend is also consistent with an improved electron delocalization with decreasing n as evidenced by spectroscopic analyses (UV–vis and IR). This finding can be of great interest for technological applications because it allows a tuning of properties of critical element like the metal/semiconductor interface which usually forms the basis of many microelectronic devices such as diodes. In order to gain further insight into the junction at such an interface, several coPPy-3CnPPy based devices were fabricated. A typical

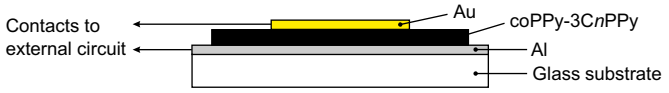

Fig. 8. Typical cross-sectional view of the fabricated Au/coPPy-3CnPPy/Al devices.

cross-sectional view of a metal/coPPy-3CnPPy/metal devices is given in Fig. 8. First, current density–voltage (J vs V) characteristics were investigated. Devices prepared from copolymers functionalized with longer alkyl chains (nonyl and undecyl) exhibit non-linear J–V curves implying a non-ohmic rectifying contact (Fig. 9), whereas that of the pentyl-based device shows a ohmic, i.e., linear, behavior. The devices showing non-linear J–V curves were further exploited by means of the Schottky barrier theory [50]. According to this theory, a p-type semi-conducting device exhibiting an asymmetric, non-ohmic (J–V) behavior can be assumed to follow the thermoionic emission process for conduction across the metal/polymer junction with the current density across the junction given by the equation:

$$J = J_0[\exp(qV/nkT) - 1], \quad (3)$$

where J is the current density per unit area, J_0 is the reverse saturation current density, q is the electronic charge, V is the applied forward bias, n is the ideality factor of the diode, k is the Boltzmann constant, and T is the absolute temperature. J_0 is given by the following equation:

$$J_0 = A^* T^2 \exp[-q\Phi_b/(kT)], \quad (4)$$

where A^* is the effective Richardson constant with a value of 120 A k^{-2} cm^{-2} for a free electron and Φ_b is the potential barrier. The above A^* value is usually assumed for Schottky diode with p-type organic semiconductor for calculations of barrier heights. At a given temperature (298 K in this work), the logarithm of J vs V of Eq. (3) is expected to provide a linear plot (inset of Fig. 9) from which the saturation current (J_0) is

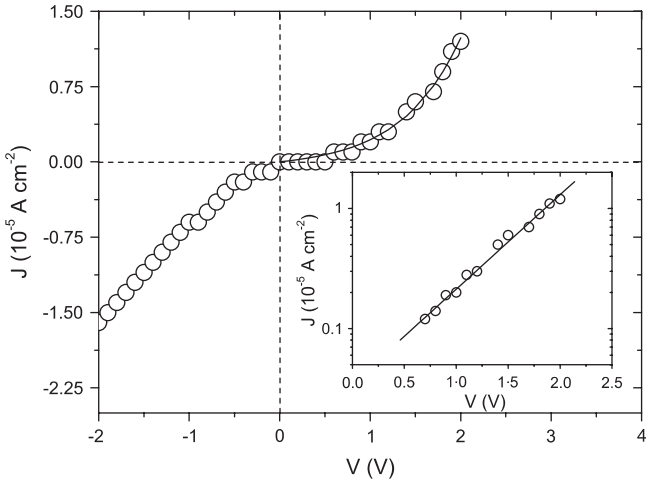

Fig. 9. Evolution of the current density J upon application of a DC voltage V for a Au/coPPy-3C*11*PPy/Al device; inset: semilogarithmic plot of J vs V.

obtained, by extrapolation, to $V = 0$ V. This linear equation is obtained when $qV/(kT) > 1$ in Eq. (3). Further, the ideality factor (n) can be deduced from the slope of the straight line region of $\log_{10} J$ vs V. The fabricated diode characteristics (J_0, Φ_b, and n) are summarized in Table 3. The estimated n values are not approaching the ideal value ($n = 1$). In this regard, it is worth mentioning that there are reported ideality values as high as 11 and 18 for junctions composed of Al/electrochemically [51] prepared tetrafluoroborate-doped (unalkylated) polypyrroles and of Al/unalkylated PPy–PET composite [52], respectively. We ascribe this discrepancy in n values to the nature of dopants, the steric effect engendered by the presence of alkyl groups and the method of polymer synthesis which affects film morphology and metal/copolymer interfacial junction properties.

One or a combination of the following arguments may be used to explain the results in Table 3. These are: (a) the presence of an insulating oxides of aluminum in-between the aluminum metal and the copolymer. Indeed, precedents on the formation of such an insulating layer on a low work function metal (aluminum) has been reported in the literature, i.e., even high vacuum (10^{-5}–10^{-6} Torr) deposition of aluminum metal on inert substrate cannot prevent the complete exclusion of oxygen [53], i.e., a thin coating of aluminum oxide was formed; (b) formation of oxidized by-products or the presence of oxygen atom containing polymers which bond with aluminum via its oxygen atom(s) thereby forming an oxide like insulating layer; (c) the absorption of oxygen by polypyrrole when exposed to air (the absorbed oxygen is not removable on pumping in vacuum [54]).

Based on the above reasons and our experimental procedures for diode fabrication (conducted in the presence of adventitious oxygen) and copolymer synthesis/processing (using water as the solvent in which dissolved oxygen was not excluded), the formation of an insulating aluminum oxide layer and/or aluminum oxide by-products cannot be ruled out. As a supporting piece of data, we found the presence of a carbonyl functional group (C=O) in the IR spectra (Fig. 4) in all synthesized copolymers indicating the formation of oxidized by-products. This by-product is known to arise from the sequence nucleophilic attack by water on the pyrrole and keto–enol tautomerization [55,56]. The oxygen terminal of the carbonyl group can readily bond with aluminum.

The electrical characteristics of coPPy-3C*n*PPy devices ($n = 9$, 11) suggest that the presence of longer alkyl chains would reduce the conjugation length in the copolymer backbone which in turn lowers the concentration of charge carrier/conductivity, thereby resulting in a wider depletion width and better junction behavior. Thus, a clear trend emerges from the J–V analyses which permits the ranking of diode performances in the following decreasing order (as a function of decreasing chain length): Au/coPPy-3C*11*PPy/Al > Au/coPPy-3C*9*PPy/Al ≫ Au/coPPy-3C*5*PPy/Al. In summary, the studies on the electrical properties demonstrate that a lower limit/threshold of alkyl chain length must be satisfied for Schottky diode behavior to take place in this series of copolymers. Investigation is underway to determine whether such a phenomenon will occur for other series of intrinsic conducting copolymers.

Table 3
Schottky diode characteristics of Al/coPPy-3C*n*PPy/Au diodes

	coPPy-3C*9*PPy	coPPy-3C*11*PPy
J_0 (A cm^{-2})	4.95×10^{-6}	7.08×10^{-7}
ϕ_b (eV)	0.73	0.78
N	86.6	25.4

4. Conclusion

The syntheses of three 3-alkyl pyrroles and their copolymerization with native pyrrole to provide the corresponding copolymers have been achieved. These copolymers revealed to be soluble in organic solvents and the resulting solutions, when coated on a substrate, produce (semi-)conducting films with a quite even surface morphology. Spectral analyses (UV–vis) showed the presence of polaronic and bipolaronic species whose bathochromic shifts and the ratio of the corresponding absorbances are linearly dependent on alkyl chain length. Likewise, IR spectral data indicate a linear correlation between the ratio of absorbances, of the hydrocarbon symmetrical and asymmetrical stretching modes, and the alkyl chain length. In addition, IR spectroscopy shows an ascending trend, in the bipolaronic, polaronic band surface areas and the corresponding ratio of the areas, with increasing alkyl chain length. The conductivity of the copolymers can be inversely correlated with alkyl chain length, i.e., the shorter the chain, the more conducting the copolymeric films. Data from electrical measurements support Schottky diode properties, although imperfect, for the nonyl- and undecyl-based diodes. However, there appears to be a threshold/lower limit in alkyl chain length below which the copolymeric film will show Ohmic behavior, and thus, cannot be used as the electroactive component for Schottky diode interface for current density rectification.

Acknowledgments

The authors are indebted to Dr. Stephane Siffert for helpful discussions on IR measurements, to Dr. Stephane Longuemart for providing Al-coated substrates, and to Dr. Lucie Courcot for carrying out SEM experiments. William Godart is acknowledged for his technical help. The authors acknowledge the Ministère de la Recherche, the CPER TAC and the CNRS for financial support. R.C.Y.K. thanks the Université du Littoral-Côte d'Opale for inviting him as a visiting Professor. He also thanks the University of Science and Arts of Oklahoma – Gladys Anderson Emerson Fund for partial financial assistance in this project. F.R. thanks the Fulbright Foundation and the Région Nord-Pas de Calais for a fellowship.

References

[1] Kim BH, Park DH, Joo J, Yu SG, Lee SH. Synth Met 2005;150(3):279.
[2] Shirakawa H. Angew Chem Int Ed 2001;40:2575.

[3] MacDiarmid AG. Angew Chem Int Ed 2001;40:2581.
[4] Heeger AJ. Angew Chem Int Ed 2001;40:2591.
[5] Cooper JM, Morris DG, Ryder KS. Langmuir 1996;12:5681.
[6] Collins CE, Buckley LJ. Synth Met 1996;78:93.
[7] Freund MS, Lewis NS. Proc Natl Acad Sci USA 1995;92:2652.
[8] Kojima T, Nishida JI, Tokito S, Tada H, Yamashita Y. Chem Commun 2007;10:1039.
[9] Horowitz G. Adv Mater 1999;10(5):365.
[10] Vozzi G, Carpi F, Mazzoldi A. Smart Mater Struct 2006;15:279.
[11] Roussel F, Chan Yu King R, Buisine JM. Eur Phys J E 2003;11:293.
[12] Wang Y, Jing X. Polym Adv Technol 2005;16(4):344.
[13] Mastragostino M, Arbizzani C, Soavi F. Solid State Ionics 2002; 148(3):493.
[14] Skotheim TA, Eisenbaumer R, Reynolds R. Handbook of conducting polymers. New York: Marcel Dekker; 1998.
[15] Costello DL, Evans BPJ, Guernion N, Ratcliffe NM, Sivanand PS, Teare GC. Synth Met 2000;114:181.
[16] MacCullough R, Lowe R, Jayaraman M, Anderson D. J Org Chem 1993; 58:904.
[17] Song M, Kim Y, Kim B, Kim J, Char K, Ree H. Synth Met 2004;141:315.
[18] Boussoualem M, Chan Yu King R, Buisine JM, Roussel F. Appl Phys A 2005;81:773.
[19] Babler JH, Spina KP. Tetrahedron Lett 1984;25:1695.
[20] Guernion N, Castillo DL, Evans BPJ, Ratcliffe NM. Synth Met 2002;128:139.
[21] Sadki S, Schottland P, Brodie N, Sabouraud G. Chem Soc Rev 2000;29:283.
[22] Constantini N, Cagnolati R, Nucci L, Pergola F, Guggeri G. Synth Met 1998;92(2):139.
[23] Chan Yu King R, Roussel F. Synth Met 2005;153:337.
[24] Omastova M, Trchova M, Korarova J, Stejskal J. Synth Met 2003; 138(3):447.
[25] Chen SA, Ni JM. Macromolecules 1992;25(23):6081.
[26] Hsu WP, Levon K, Ho KS, Myerson AS, Kwei TK. Macromolecules 1993;26:1318.
[27] Kim DY, Lee JY, Kim CY, Kang ET, Tan KL. Synth Met 1995;72:243.
[28] Bredas JL, Scott JC, Yakushi K, Street GB. Phys Rev B 1984;30:1023.
[29] Scott JC, Bredas JL, Yakushi K, Pfluger P, Street GB. Synth Met 1984;9:165.
[30] Bredas JL, Themans, Fripia JG, Andre JM, Chance RR. Phys Rev B 1984;29:6761.
[31] Havinga EE, Hoeve WT, Meijer EW, Wynberg H. Chem Mater 1989;1:650.
[32] Masuda H, Tanaka S, Kaeriyama K. J Polym Sci Part A Polym Chem 1990;28:1831.
[33] Kaeriyama K, Masuda H. Synth Met 1991;41–43:389.
[34] Davidson RG, Turner TG. Synth Met 1995;72:121.
[35] Genies EM, Boyle A, Lapkowski M, Tsintavis C. Synth Met 1990; 36:139.
[36] Yakushi K, Lauchlan LJ, Clarke TC, Street JB. J Chem Phys 1983; 79:4774.
[37] Snyder RG, Strauss HL, Elliger CA. J Phys Chem 1982;86:5145.
[38] Bredas JL, Stret GB. Acc Chem Res 1985;18:309.
[39] Bantikassegn W, Inganas O. J Phys D Appl Phys 1996;29:2971.
[40] Tian B, Zerbi G. J Chem Phys 1990;92:3886.
[41] Tian B, Zerbi G. J Chem Phys 1990;92:3892.
[42] Tian B, Zerbi G. J Electroanal Chem 1990;92(6):3892.
[43] Aguilar-Hernandez J, Potje-Kamloth K. J Phys D Appl Phys 2001; 34:1700.
[44] Subramanyam VS, Das SK, Ganguly BN, Battacharya A, De A. Mater Res Bull 1997;32(8):1063.
[45] Mott NF. Adv Phys 1967;16:49.
[46] Mott NF. Philos Mag 1969;19:835.
[47] Mott NF, Davis EA. Electronic processes in noncrystalline materials. Oxford: Clarendon; 1979. p. 324.
[48] Paul DK, Mitra SS. Phys Rev Lett 1973;31:1000.
[49] Nair K, Mitra SS. J Non-Cryst Solids 1977;24:1.
[50] Sze SM. Physics of semiconductor devices. NY: Wiley; 1981.
[51] Gupta R, Misra SCK, Malhotra BD, Belakadere NN, Chandra S. Appl Phys Lett 1991;58:51.
[52] Li C, Song Z. Synth Met 1991;44:159.
[53] Inganas O, Lundstrom I. Synth Met 1984;10:5.
[54] Scott JC, Pfluger P, Krounbi MT, Street JB. Phys Rev B 1983;28: 2140.
[55] Maia G, Ticianelli EA, Nart FC. Z Phys Chem 1994;186:245.
[56] Prissanaroon W, Ruangchuay L, Sirivat A, Schwank J. Synth Met 2000; 114:65.